World Academy of Science, Engineering and Technology
International Journal of Mechanical and Mechatronics Engineering
Vol:10, No:1, 2016

Numerical Simulation of a Three-Dimensional Framework under the Action of Two-Dimensional Moving Loads

Jia-Jang Wu

International Science Index, Mechanical and Mechatronics Engineering Vol:10, No:1, 2016 waset.org/Publication/10003446

***Abstract*—**The objective of this research is to develop a general technique so that one may predict the dynamic behaviour of a three-dimensional scale crane model subjected to time-dependent moving point forces by means of conventional finite element computer packages. To this end, the whole scale crane model is divided into two parts: the stationary framework and the moving substructure. In such a case, the dynamic responses of a scale crane model can be predicted from the forced vibration responses of the stationary framework due to actions of the four time-dependent moving point forces induced by the moving substructure. Since the magnitudes and positions of the moving point forces are dependent on the relative positions between the trolley, moving substructure and the stationary framework, it can be found from the numerical results that the time histories for the moving speeds of the moving substructure and the trolley are the key factors affecting the dynamic responses of the scale crane model.

***Keywords*—**Moving load, moving substructure, dynamic responses, forced vibration responses.

I. Introduction

THE scale crane model investigated herein is a fabricated structure [1], which consists of several parts: (1) the stationary framework, (2) the moving rails, (3) the overhead trolley and (4) the spreader, as shown in Fig. 1. The overhead trolley runs on the moving rails and the moving rails move along the two parallel beams (or fixed rails) on the top of the stationary framework. In order to predict the dynamic characteristics of the scale crane model due to the movements of the moving rails and the overhead trolley, it is required to determine the excitations on the scale crane model induced by the moving rails and the overhead trolley. Thus, the dynamic characteristics of a scale crane model can be predicted from the forced vibration responses of the stationary framework due to actions of the concentrated forces located at the four contacting points between the stationary framework and the moving substructure.

Existing standard finite element computer packages, such as I-DEAS [2], [3] are not usually set up to easily accommodate time-dependent, moving, loads. Therefore, by means of a finite element package for solving the moving-force-induced vibration problem, it requires the replacement of the moving force(s) by equivalent nodal force vector(s) at any instant of time. To this end, the fundamental principle used is to apply forces and moments to all the nodes of the finite element model of the structure, making these forces and moments functions of time. In order to develop techniques for deriving appropriate force/time and moment/time functions for all the nodes on a structure, a beam subjected to a single moving concentrated force is initially studied [4]-[11]. Then, it is extended to deal with a pair of beams, each of them subjected to two time-dependent moving concentrated forces. This approach may be applied to the dynamic analysis of the scale crane model.

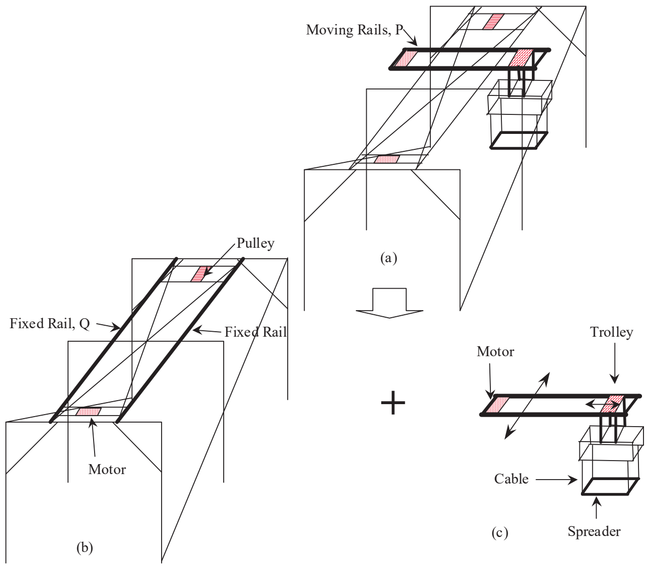

Fig. 1 The scale crane model: (a) whole structure, (b) stationary framework and (c) moving substructure (the rotating motor and hoisting motor are not shown)

II. Derivation of Contact Point Forces Induced by the Moving Substructure and Trolley

According to the substructure theory, the whole scale crane structure can be divided into two parts: the stationary framework and the moving substructure. Fig. 1 shows the moving substructure consisting of two moving rails, a moving trolley, and a spreader. The whole structure, the stationary framework, and the moving substructure are shown in Figs. 1 (a)-(c). Fig. 2 (a) shows the concentrated forces ($F_{z1}(t)$ and $F_{z2}(t)$) at the four contact points (A, B, C and D) and the relevant symbols (e.g., $0, \bar{x}, \bar{y}, \bar{z}$, $C_x(t)$, $C_y(t)$ … $V_{cx}(t)$ and

Jia-Jang Wu is with the Department of Marine Engineering, National Kaohsiung Marine University, No. 482, Jhong-Jhou 3rd Road, Cijin District, Kaohsiung City 80543, Taiwan (phone: 886-7-810-0888 ext. 5230; fax: 886-7-572-1035; e-mail: jjangwu@mail.nkmu.edu.tw).

$V_{cy}(t)$) for the scale crane model structure [1]. The moving substructure may move on the two fixed rails Q along the $\bar{y}$ axis and the trolley may move on the two moving rails P along the $\bar{x}$ axis. A, B, C and D are the four points of contact between the two substructures. Fig. 2 (b) shows the free-body diagram for each of the two moving rails P. From Fig. 2 (a), it can be found that the centreline of the moving substructure parallel to the $\bar{x}$ axis is a *symmetric axis* for the whole moving substructure. Hence, the interactive forces between the two fixed rails and one of the two moving rails are equal to the corresponding forces between the two fixed rails and the other one of the two moving rails. This is the reason why the contact force at point A is equal to that at point B (i.e., $F_{zA}(t) = F_{zB}(t) = F_{z1}(t)$), and the contact force at point D is equal to that at point C (i.e., $F_{zD}(t) = F_{zC}(t) = F_{z2}(t)$) as shown in Fig. 2(a). Each contact force (either F_{z1} (t) or $F_{z2}(t)$) may be divided into two components. One of them is due to the weight of the whole moving substructure (Fig. 1 (c)), excluding the weight of the moving trolley together with the spreader and the hoisted container. This component maintains a constant magnitude but changes its position when the whole substructure moves in the $\bar{y}$ direction along the two fixed rails. The other component is due to the moving trolley together with the spreader and the hoisted container. This component changes its magnitude when the trolley moves in the direction parallel to the $\bar{x}$ axis along the two moving rails. The summation of the two contact force components mentioned above and the excitations due to the drive motors defines the instantaneous magnitude of each contact point force. The instantaneous positions of the four contact point forces are determined by the relative position between the two moving rails (on the moving substructure) and the two fixed rails (on the top of the stationary framework).

According to the principle of moment equilibrium, for point Z1 as shown in Fig. 2 (b), one has

$$\sum M_{Z1} = -(\tfrac{1}{2} m_{mot} g + \tfrac{1}{2} F_{e1} \sin(\omega_{e1} t))(x_{mot} - \tfrac{x_a}{2}) + (\tfrac{1}{2} m_p g)(\tfrac{1}{2} x_a) - F_{Z2}(t) x_a + (\tfrac{1}{2} m_c g)(C_x(t) + \tfrac{1}{2} x_a) = 0$$

or

$$F_{Z2}(t) = \tfrac{1}{4} m_p g + \tfrac{1}{4} m_c g (1 + 2(\tfrac{C_x(t)}{x_a})) + \tfrac{1}{2}(m_{mot} g + F_{e1} \sin(\omega_{e1} t))(\tfrac{1}{2} - \tfrac{x_{mot}}{x_a}) \quad (1)$$

Similarly, for point Z2 as shown in Fig. 2 (b), one has

$$\sum M_{Z2} = -(\tfrac{1}{2} m_{mot} g + \tfrac{1}{2} F_{e1} \sin(\omega_{e1} t))(x_{mot} + \tfrac{x_a}{2}) + F_{Z1}(t) x_a - (\tfrac{1}{2} m_p g)(\tfrac{1}{2} x_a) + (\tfrac{1}{2} m_c g)(C_x(t) - \tfrac{1}{2} x_a) = 0$$

or

$$F_{Z1}(t) = \tfrac{1}{4} m_p g + \tfrac{1}{4} m_c g (1 - 2(\tfrac{C_x(t)}{x_a})) + \tfrac{1}{2}(m_{mot} g + F_{e1} \sin(\omega_{e1} t))(\tfrac{1}{2} + \tfrac{x_{mot}}{x_a}) \quad (2)$$

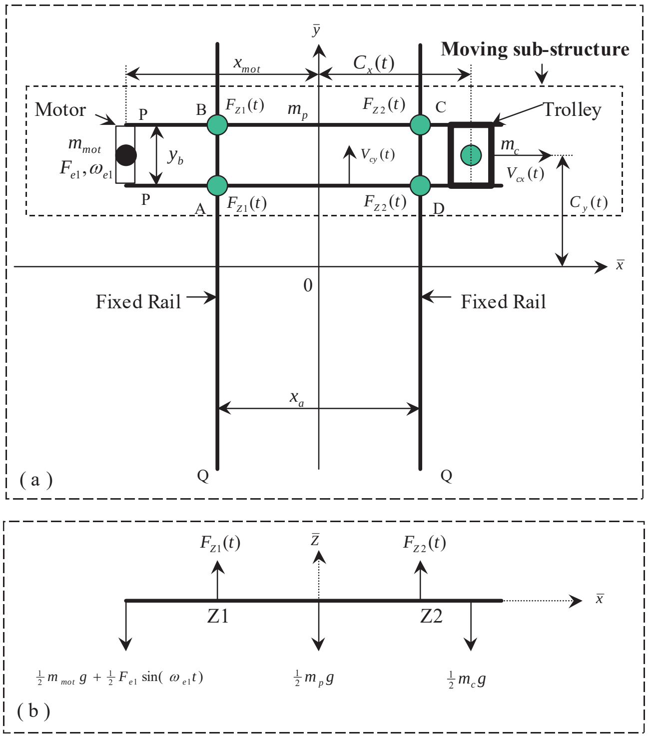

Fig. 2 (a) Contact point forces on the moving rails ($F_{z1}(t)$ and $F_{z2}(t)$) and the relevant symbols; (b) Free-body diagram for each of the two moving rails P

If the excitation due to the motor is negligible, i.e., $F_{e1} = 0$, then (1) and (2) reduce to

$$F_{Z2}(t) = \tfrac{1}{4} m_p g + \tfrac{1}{4} m_c g (1 + 2(\tfrac{C_x(t)}{x_a})) + \tfrac{1}{2} m_{mot} g (\tfrac{1}{2} - \tfrac{x_{mot}}{x_a}) \quad (3)$$

$$F_{Z1}(t) = \tfrac{1}{4} m_p g + \tfrac{1}{4} m_c g (1 - 2(\tfrac{C_x(t)}{x_a})) + \tfrac{1}{2} m_{mot} g (\tfrac{1}{2} + \tfrac{x_{mot}}{x_a}) \quad (4)$$

where

$$C_x(t) = C_{x0} + V_{cx0} t + \tfrac{1}{2} a_{cx} t^2 \quad (5a)$$

or

$$C_x(t) = C_{x0} + V_{cx0} t_x + \tfrac{1}{2} a_{cx} t_x{}^2 + V_{cxmax}(t - t_x) \quad (5b)$$

$$t_x = (V_{cxmax} - V_{cx0}) / a_{cx} \quad (6)$$

where C_{x0} and $C_x(t)$ represent the *initial* and the *instantaneous* $\bar{x}$ co-ordinates for the centre of the trolley, respectively. V_{cx0} and V_{cxmax} represent the *initial* and the *maximum* speeds of the trolley along the $\bar{x}$ axis, a_{cx} represents the acceleration of the trolley, and t_x represents the time that the trolley takes to accelerate from V_{cx0} to V_{cxmax} . It is noted that all the subscripts x for the foregoing symbols represent "along the $\bar{x}$ axis". Equation (5a) represents the instantaneous $\bar{x}$ co-ordinate, $C_x(t)$, for the trolley continuously accelerating along the $\bar{x}$ axis and (5b) represents that for the trolley accelerating to the maximum speed V_{cxmax} and then moving at this maximum speed along the $\bar{x}$ axis.

Since the forces given by (3) and (4), $F_{Z1}(t)$ and $F_{Z2}(t)$, represent the forces acting on the two moving rails, P, the forces acting on the two fixed rails, Q, are those of the same magnitudes but in opposite directions, i.e.,

$$F_{Z2}(t) = -\tfrac{1}{4} m_p g - \tfrac{1}{4} m_c g (1 + 2(\tfrac{C_x(t)}{x_a})) - \tfrac{1}{2} m_{mot} g (\tfrac{1}{2} - \tfrac{x_{mot}}{x_a}) \quad (7)$$

$$F_{Z1}(t) = -\tfrac{1}{4} m_p g - \tfrac{1}{4} m_c g (1 - 2(\tfrac{C_x(t)}{x_a})) - \tfrac{1}{2} m_{mot} g (\tfrac{1}{2} + \tfrac{x_{mot}}{x_a}) \quad (8)$$

III. Calculation of $\bar{y}$ co-Ordinates for the Nodes at which the Contact Point Forces are Located

As shown in Fig. 2 (a), the moving substructure moves on the two fixed rails along the $\bar{y}$ axis, hence the $\bar{y}$ co-ordinates of the four contact points, A, B, C and D, vary with time. In order to define the instantaneous $\bar{y}$ co-ordinates of the four contact points it is necessary to calculate the position of the centreline of the moving substructure (or the centre of the trolley) at time t, $C_y(t)$.

If the moving substructure (or the trolley) moves along the $\bar{y}$ axis with a constant acceleration a_{cy}, then

$$C_y(t) = C_{y0} + V_{cy0}\, t + \tfrac{1}{2} a_{cy}\, t^2 \quad (9)$$

where C_{y0} and V_{cy0} are the initial displacement and velocity of the moving substructure (or the trolley), respectively. If the moving substructure accelerates along the $\bar{y}$ axis to the maximum speed V_{cymax} and then moves with that speed, then

$$C_y(t) = C_{y0} + V_{cy0}\, t_y + \tfrac{1}{2} a_{cy}\, t_y^{\,2} + V_{cymax}\,(t - t_y) \quad (10)$$

$$t_y = \frac{V_{cymax} - V_{cy0}}{a_{cy}} \quad (11)$$

After the instantaneous position, $C_y(t)$, for the centreline of the moving substructure (or the centre of the trolley) is determined, the $\bar{y}$ co-ordinates for the four contact points, A, B, C and D, $\bar{y}_A(t)$, $\bar{y}_B(t)$, $\bar{y}_C(t)$ and $\bar{y}_D(t)$, are easily calculated:

$$\bar{y}_A(t) = C_y(t) - \tfrac{y_b}{2} \quad (12)$$

$$\bar{y}_B(t) = C_y(t) + \tfrac{y_b}{2} \quad (13)$$

$$\bar{y}_C(t) = C_y(t) + \tfrac{y_b}{2} \quad (14)$$

$$\bar{y}_D(t) = C_y(t) - \tfrac{y_b}{2} \quad (15)$$

where y_b is the spacing of the two moving rails P, as shown in Fig. 2 (a).

IV. Forced Vibration of a Beam Subjected to a Single Moving Point Force

A. The Overall Equivalent Nodal Force Vector

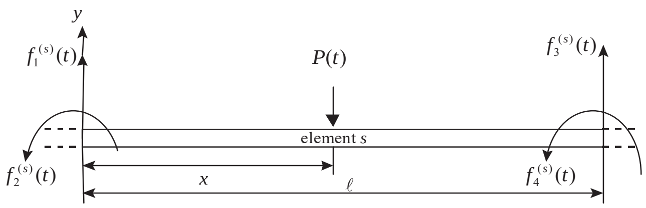

Fig. 3 Equivalent nodal forces $f_i^{(s)}(t)$ (i = 1 to 4) for the beam element, s, on which a concentrated force $P(t)$ applies

The equation of motion for a multiple degree-of-freedom linear structural system is given by

$$[M]\{\ddot{q}(t)\} + [C]\{\dot{q}(t)\} + [K]\{q(t)\} = \{F(t)\} \quad (16)$$

where [M], [C] and [K] are the overall mass, damping and stiffness matrices, respectively, and $\{\ddot{q}(t)\}$, $\{\dot{q}(t)\}$ and $\{q(t)\}$ are the overall acceleration, velocity and displacement vectors, respectively, while $\{F(t)\}$ is the overall external force vector.

When a beam is subjected to a concentrated force, $P(t)$, all the nodal forces of the beam are equal to zero except those for the beam element, s, on which the concentrated force $P(t)$ applies (Fig. 3) [4]-[11]. Hence, the overall external force vector $\{F(t)\}$ in (16) takes the form

$$\{F(t)\} = [0\,0\,0 \cdots f_1^{(s)}(t)\; f_2^{(s)}(t)\; f_3^{(s)}(t)\; f_4^{(s)}(t) \cdots 0\,0\,0]^T \quad (17)$$

where $f_i^{(s)}(t)$ (i = 1 to 4) are the equivalent nodal forces for the beam element, s, and are given by

$$\begin{Bmatrix} f_1^{(s)}(t) \\ f_2^{(s)}(t) \\ f_3^{(s)}(t) \\ f_4^{(s)}(t) \end{Bmatrix} = P(t) \begin{Bmatrix} N_1(\zeta) \\ N_2(\zeta) \\ N_3(\zeta) \\ N_4(\zeta \end{Bmatrix} \quad (18)$$

where $N_i(\zeta)$ (i = 1 to 4) represent the shape functions given by [12]

$$N_1(\zeta) = 1 - 3\zeta^2 + 2\zeta^3 \quad (19a)$$

$$N_2(\zeta) = (\zeta - 2\zeta^2 + \zeta^3) \cdot \ell \quad (19b)$$

$$N_3(\zeta) = 3\zeta^2 - 2\zeta^3 \quad (19c)$$

$$N_4(\zeta) = (-\zeta^2 + \zeta^3) \cdot \ell \quad (19d)$$

$$\zeta = \frac{x}{\ell} \quad (19e)$$

B. Equivalent Nodal Forces Due to a Moving Point Force

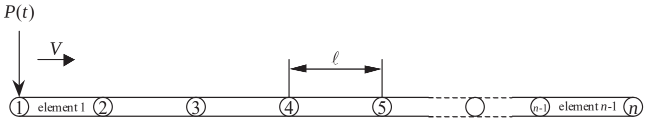

Fig. 4 Beam subjected to a concentrated force $P(t)$ moving with a constant speed V

Fig. 4 shows a beam composed of n nodes and n-1 beam elements. If a concentrated force $P(t)$ moves from node 1 to node n of the beam with a constant speed V, then the relationship between the time interval, Δt, total time steps, q, and the time duration required for the force to run over the beam, t_{max}, is given by

$$t_{max} = q\,\Delta t \quad (20)$$

The force and moment vectors contain the force and moment information for all nodes on the beam at all time steps:

$$\{F_t^i\}_{q+1} = [F_{t=0}^i \quad F_{t=\Delta t}^i \quad F_{t=2\Delta t}^i \quad \cdots \quad F_{t=q\Delta t}^i]^T \text{ , } i = 1 \text{ to } n \quad (21)$$

$$\{M_t^i\}_{q+1} = [M_{t=0}^i \quad M_{t=\Delta t}^i \quad M_{t=2\Delta t}^i \quad \cdots \quad M_{t=q\Delta t}^i]^T \text{ , } i = 1 \text{ to } n \quad (22)$$

where i represents the node number.

At time $t = 0$, the concentrated force is at node 1, as shown in Fig. 4,

$$F_{t=0}^1 = P(t) \text{ , } F_{t=0}^i = 0 \;\; (i = 2 \text{ to } n) \text{ and } M_{t=0}^i = 0 \;\; (i = 1 \text{ to } n) \quad (23)$$

At any time $t = r\,\Delta t$ (r = 1 to q), the position of the moving concentrated force, relative to the left end of the beam, is given by

$$x_p(t) = V\,r\,\Delta t \quad (24)$$

The numerical identification of the beam element, s, on which the moving concentrated force, $P(t)$, is applied, at any time t, is determined by

$$s = (\text{The integer part of } \frac{x_p(t)}{\ell}) + 1 \quad (25)$$

where ℓ is the length of each beam element (Fig. 4).

The two nodes of the s^{th} (s = 1 to n-1) beam element are s and s+1. Therefore, the nodal forces and moments when the moving concentrated force, $P(t)$, is on the s^{th} beam element at any time $t = r\Delta t$ (r = 1 to q) are given by

$$F_{t=r\Delta t}^s = P(t)\,N_1(\zeta_P) \quad (26)$$

$$F_{t=r\Delta t}^{s+1} = P(t)\,N_3(\zeta_P) \quad (27)$$

$$F_{t=r\Delta t}^i = 0\,(i = 1 \text{ to } n\,;\, i \neq s \text{ and } s+1) \quad (28)$$

$$M_{t=r\Delta t}^s = P(t)\,N_2(\zeta_P) \quad (29)$$

$$M_{t=r\Delta t}^{s+1} = P(t)\,N_4(\zeta_P) \quad (30)$$

$$M_{t=r\Delta t}^i = 0 \;\; (i = 1 \text{ to } n\,;\; i \neq s \text{ and } s+1) \quad (31)$$

$$\zeta_P = \frac{x_p(t) - (s-1)\ell}{\ell} \quad (32)$$

and $N_i(\zeta_p) = \psi_i(\zeta)$, ($i$ = 1 to 4), are the shape functions defined by (19).

V. Numerical Examples

A. Validation

To confirm the technique that has been developed, a uniform undamped simply supported beam of length L = 1 m and cross section A = 2 $cm \times 1$ cm with 10 beam elements (i.e., n = 11) is investigated using I-DEAS. The beam is made of steel with density ρ = 7820 kg/m^3 and modulus of elasticity E = 206.8 GN/m^2. At the instant of time t = 0, a vertical point force $P(t)$ = sin (10 t) N starts to move from the left end to the right end with a constant speed V = 1 m/s. In order to perform the forced vibration analysis of the simply supported beam subjected to a moving harmonic force, a finite element model of the simply supported beam is established, as shown in Fig 5. The time-dependent nodal forces and moments for all the nodes of the finite element model are obtained by means of the self-developed FORTRAN program, as shown in Fig. 6. The time histories of the vertical central displacements (at $x = L/2$) of the simply supported beam obtained from the foregoing dynamic-analysis methods are shown in Fig. 7. It is seen that the results determined by I-DEAS are in good agreement with those obtained from the two analytical closed-form solutions. So, the Finite Element method has been shown to be appropriate in this research.

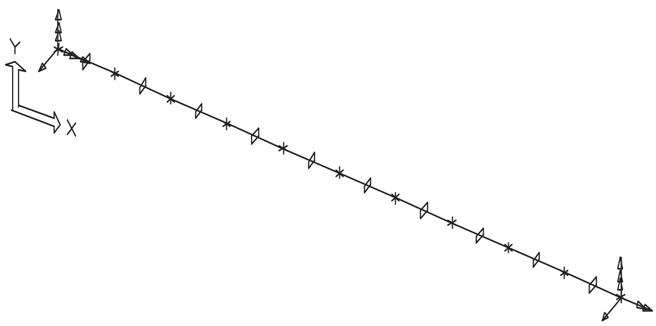

Fig. 5 Finite element model of a simply supported beam for I-DEAS

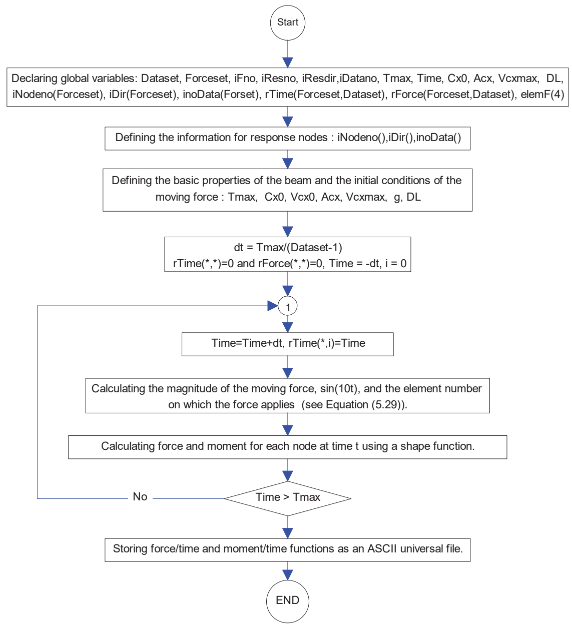

Fig. 6 Flowchart of the computer program for calculating the time-dependent nodal forces and moments, and storing the related information as an ASCII universal file to be read by I-DEAS

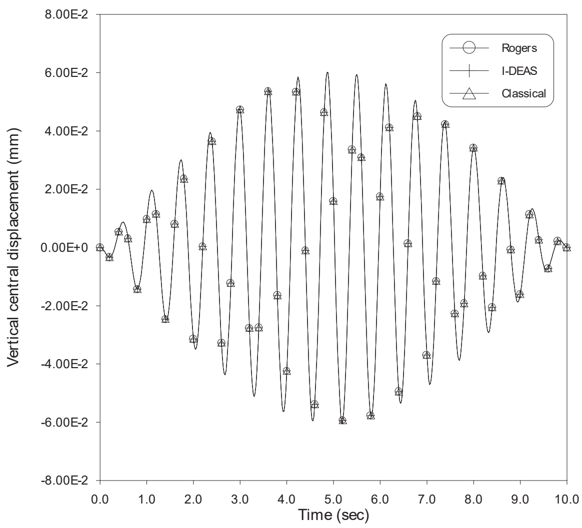

Fig. 7 Time histories for the vertical central displacements (at $x = L/2$) of the simply supported beam obtained from the I-DEAS (---+---), classical method (—Δ—) and Rogers' method (—O—)

B. Dynamic Analysis of the Scale Crane Model

Fig. 8 shows the scale model for a mobile crane, where the whole system is divided into two parts: the stationary framework and the moving substructure. The dynamic behaviour of the whole system is determined by the forced vibration responses of the stationary framework subjected to four concentrated time-dependent moving forces induced by the substructure moving in the $\bar{y}$ direction, and the trolley moving in the $\bar{x}$ direction.

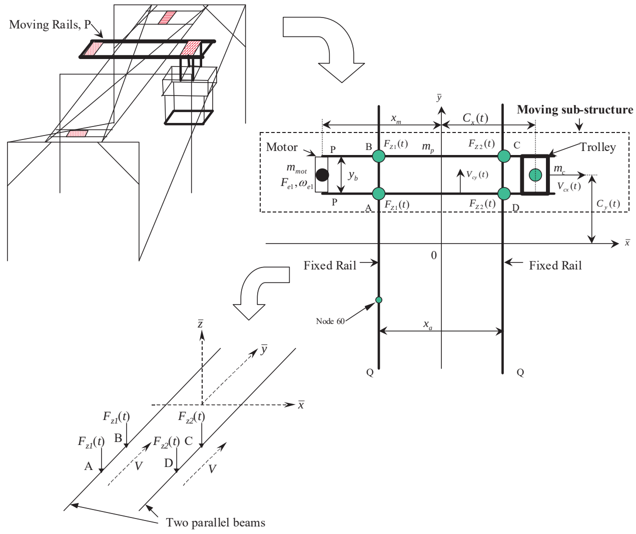

Fig. 8 Sketch of the scale model of a mobile crane studied

Time t (s)	0	→	1.0	→	2.5	→	3.0	→	3.5	→	4.0	→	10.0
$\bar{y}$ (m) *	–0.60	→	→	→	→	→	→	→	•	•	•	•	0.709
$\bar{x}$ (m) *	–0.49	→	→	→	→	→	→	→	→	→	•	•	0.4472
$V_{cy}(t)$ (m/s)	0	Accelerate	0.5236			Decelerate			Stationary (0)				
$V_{cx}(t)$ (m/s)	0	Accelerate	0.3142					Decelerate				Stationary (0)	
$a_{cy}(t)$ (m/s²)**	-------	+0.5236	0			–0.5236				0			
$a_{cx}(t)$ (m/s²)**	-------	+0.3142	0					–0.3142				0	

* → denotes moving and • denotes stationary.
** + denotes acceleration and – denotes deceleration.

Fig. 9 Time histories for the moving speeds of the moving substructure ($V_{cy}(t)$) and the trolley ($V_{cx}(t)$)

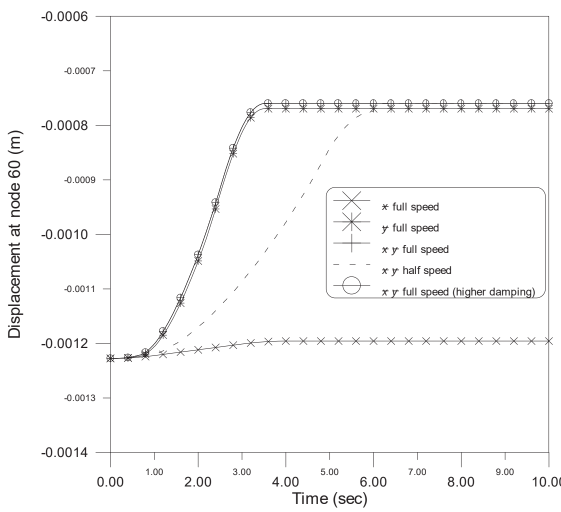

Fig. 10 Time histories of the vertical displacements of node 60, $\bar{z}_{60}(t)$

In the present example, the initial position and the final position, and the accelerating and decelerating conditions of the trolley, are all listed in Fig. 9. It is noted that the positive sign (+) denotes acceleration and the negative sign (–) denotes deceleration. The magnitudes of the accelerations, or decelerations, in a specified period are constant. For example, during the interval $0 < t \leq 1.0$ s, the acceleration of the moving substructure is a_{cy} = +0.5236 m/s^2, and is a constant. For the example under discussion, the accelerations, or decelerations, in different intervals of time are equal to each other, i.e., $|a_{cy}| = |+0.5236| = |-0.5236|$ m/s^2. Unless specifically stated the damping ratio (for each mode) is $\xi = 0.003$ in this work.

For the finite element model of the scale crane rig when it is subjected to time-dependent contacting forces induced by the moving substructure and the trolley moving generally, as shown in Fig. 9, the time histories of the displacements of node 60 on the fixed railway of the stationary framework (Fig. 8), $\bar{z}_{60}(t)$ (*m*), are shown in Fig. 10. The curve with + is for the case for damping ratio ξ = 0.003, and the curve with O is for ξ = 0.01. Because these two curves are coincident with each other the damping effect appears to be negligible in this example in the non-resonant condition. The dashed curve (without any symbol) is obtained under the condition when the velocities of the moving substructure are equal to half of the corresponding values used for the other two curves, respectively. It is evident that the time taken for the former two curves is twice that which is required for the dashed curve to reach its maximum.

In the special case where the trolley is stationary (i.e., $V_{cx}(t)$ = 0), and the moving substructure moves with velocities $V_{cy}(t)$ according to the data given in Fig. 9, the time history of $\bar{z}_{60}(t)$ is shown in Fig. 10 by the curve with $\ast$. It is seen that this curve is very close to the two former curves with symbols + and O. This means that the influence of trolley motion is not really significant in this example. Another special case is when the substructure is stationary (i.e.,$V_{cy}(t)$ = 0), but the trolley is moving with velocities $V_{cx}(t)$, according to the conditions given in Fig. 9. For this case the time history of $\bar{z}_{60}(t)$ is shown in Fig. 10 by the curve with $\times$. From Fig. 10 one sees that the curve looks like a horizontal line, which agrees with the last conclusion that the influence of trolley motion is not significant in this particular example. It should be noted that the superposition of the last two curves (with symbols $\ast$ and $\times$) is coincident with the former two curves (with symbols + and O) as one would expect.

VI. Conclusions

A technique has been developed for using standard finite element packages to analyse the dynamic response of structures subjected to time-dependent moving forces. A computer program has been designed to calculate the time-dependent external nodal forces on the whole structure, and which provides the equivalent nodal forces induced by point forces moving around the structure.

Acknowledgements

This work was supported by the Ministry of Science and Technology, the Republic of China, under contract No. MOST 104-2221-E-022-012.

References

[1] J. J. Wu 2011 *Development of the graphical user interface for the computerisation of a mobile gantry crane*. Technique report, National Kaohsiung Marine University, Kaohsiung, Taiwan.
[2] SDRC 2006 *I-DEAS Master Series 10 User's Guide*. Structural Dynamics Research Corporation.
[3] SDRC 2006 *I-DEAS Master Series 10 Finite Element Modeling*. Structural Dynamics Research Corporation.
[4] J. S. Wu and C. W. Dai 1987 *Journal of Structural Engineering* 113(3), 458-474. Dynamic responses of multi-span non-uniform beam due to moving loads.
[5] H. P. Lee *Computers & Structures* 1995 55(4), 615-623. Dynamic response of a multi-span beam on one-side point constraints subject to a moving load.
[6] T. P. Chang and Y. N. Liu 1996 *International Journal of Solids and Structures* 33(12), 1673-1688. Dynamic finite element analysis of a nonlinear beam subjected to a moving load.
[7] D. Thambiratnam and Y. Zhuge 1996 *Journal of Sound and Vibration* 198(2), 149-169. Dynamic analysis of beams on an elastic foundation subjected to moving loads.
[8] J. S. Wu and K.Z. Chen 1995 *Journal of Sound and Vibration* 188(3), 337-345. Dynamic analysis of a channel beam due to a moving load.
[9] Y. H. Lin 1995 *Journal of Sound and Vibration* 180(5), 809-812. Comments on "Dynamic response of a beam with intermediate point constraints subject to a moving load".
[10] C. K. Karaolodes and A. N. Kounadis 1983 *Journal of Sound and Vibration* 88(1), 37-45. Forced motion of a simple frame subjected to a moving force.
[11] M. Olsson 1985 *Journal of Sound and Vibration* 99(1), 1-12. Finite element modal co-ordinate analysis of structures subjected to moving loads.
[12] R. W. Clough and J. Penzien 1993 *Dynamics of Structures*, 2nd Edition, McGraw-Hill, New York.